Nanoscale

Supporting Information

Surface Passivation and Self-Regulated Shell Growth in Selective Area-Grown GaN-(Al,Ga)N Core-Shell Nanowires

Martin Hetzl,*[a] Julia Winnerl,[a] Luca Francaviglia,[b] Max Kraut,[a] Markus Döblinger,[c] Sonja Matich,[a] Anna Fontcuberta i Morral,[b] and Martin Stutzmann[a]

1 Numerical simulations of the electron density

In order to assess the influence of unintentional n-type doping by interdiffusing Si from the substrate, numerical band structure simulations have been performed by Nextnano[3].[1] This software solves the Poisson and drift-diffusion-current equation self-consistently in a Newton-Raphson algorithm. In Figure 1a, the

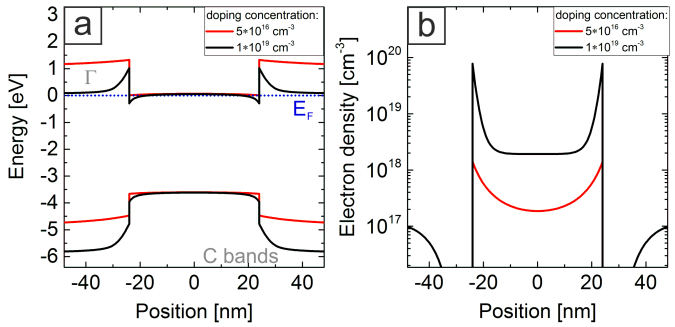

Fig. 1 (a) Electronic band structure of the GaN-(Al,Ga)N core-shell NW cross section for different doping concentrations and (b) corresponding electron density.

electronic band structures over the nanowire (NW) cross section for a quasi intrinsic (red curves) and a highly doped (black curves) GaN-(Al,Ga)N core-shell NW are plotted. With higher doping concentration, a more pronounced band bending occurs at the GaN/(Al,Ga)N interface. This leads to a separation of charge carriers, namely conduction band electrons toward the interface and valence band holes toward the center of the GaN core. However, due to the high doping concentration also in the GaN, a large number of electrons is still present at the center of the core (Fig.1b, black curve). In particular, the electron density of the higher doped core-shell NW even exceeds the low doped case by one order of magnitude. Thus, enough charge carriers are present within the center of the core allowing direct recombination with holes from the GaN valence band. This excludes a doping effect to be the origin for the intensity drop observed in photoluminescence (PL) measurements.

2 Wavelength-dependent CL detection

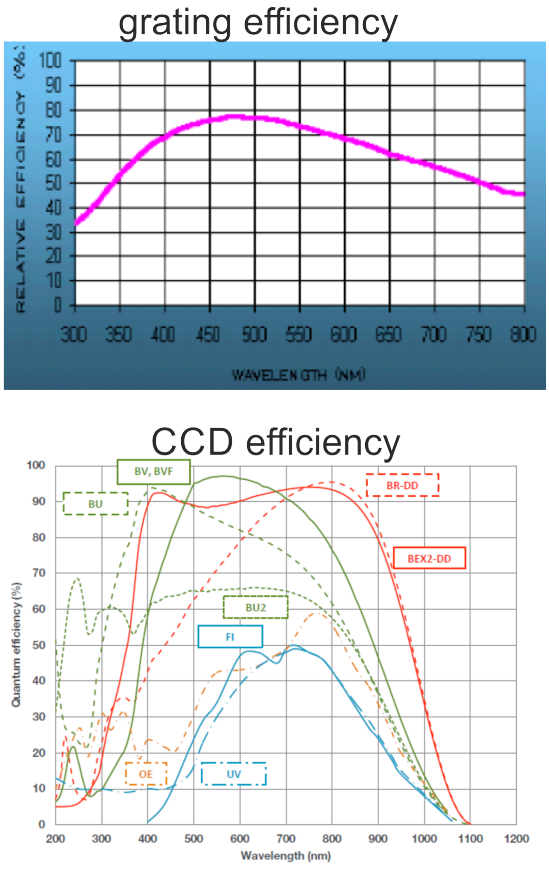

Fig. 2 (Top) Efficiency of the grating used for CL detection (150 l/mm, 500 nm blaze). (Bottom) Quantum efficiencies of different CCD cameras. The curve for the CCD used is labeled with BEX2-DD and is plotted as a red solid line.

In Figure 2 (top), the efficiency of the grating used for

* E-mail: martin.hetzl@wsi.tum.de; stutz@wsi.tum.de
[a] *Walter Schottky Institut and Physics Department, Technische Universität München, 85748 Garching, Germany.*
[b] *Laboratoire des Matériaux Semiconducteurs, École Polytechnique Fédérale de Lausanne, 1015 Lausanne, Switzerland*
[c] *Department of Chemistry, Ludwig-Maximilians-Universität München, 81377 Munich, Germany.*

cathodoluminescence detection is plotted as a function of the wavelength. A maximum efficiency of 80% can be achieved at around 500 nm (≈2.5 eV) and drops to ≈50% for 350 nm (≈3.5 eV). Moreover, the efficiencies of the CCD camera used are ≈90% and ≈45% for the mentioned wavelengths, respectively (Fig.2 bottom). Transferred to the CL measurements in the main article, this leads to an overestimation of the yellow luminescence (YL) compared to the $X_{A,C}$ emission by a factor of three to four.

3 CL spectra of GaN and GaN-(Al,Ga)N core-shell NWs on Si

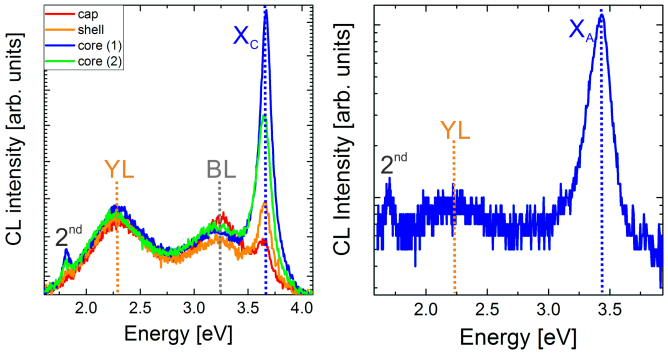

Fig. 3 (Left) CL spectra of distinct sites along a GaN-(Al,Ga)N core-shell NW. The curves represent the vertically unshifted data of Figure 3b in the main article. (Right) CL spectrum of self-assembled GaN NWs on Si.

In Figure 3 (left) CL spectra of the (Al,Ga)N cap, the (Al,Ga)N shell and two distinct sites of the GaN core are displayed in the case of a GaN-(Al,Ga)N core-shell NW, released from a Si substrate, with a core diameter of 69 nm and a shell thickness of 46 nm. The respective curves are equivalent to those in Figure 3b in the main article with, however, no vertical shift. By comparing the spectra acquired close to the core and the shell, the YL of GaN remains at a similar intensity whereas the excitonic recombination of GaN (X_C) decreases. This indicates that YL is predominantly emitted from the GaN NW surface. Moreover, the defect-related blue luminescence (BL) in (Al,Ga)N is more pronounced in the cap compared to the shell. This indicates a higher density of corresponding defects within the (Al,Ga)N cap. In Figure 3 (right) the CL spectrum of bare self-assembled GaN NWs on Si is plotted. The YL of self-assembled GaN NWs is much lower compared to bare SAG GaN NWs on Si (main article), which indicates a higher density of surface defects for SAG GaN NWs.

4 CL spectra of GaN-(Al,Ga)N core-shell NWs on diamond

In Figure 4, CL spectra of distinct sites, a SEM image and false-colored CL maps of a released GaN-(Al,Ga)N core-shell NW grown on diamond substrate are displayed. Note that in the upper right corner, a so-called tripod structure is also visible, which can arise from an incorrect nucleation process in this

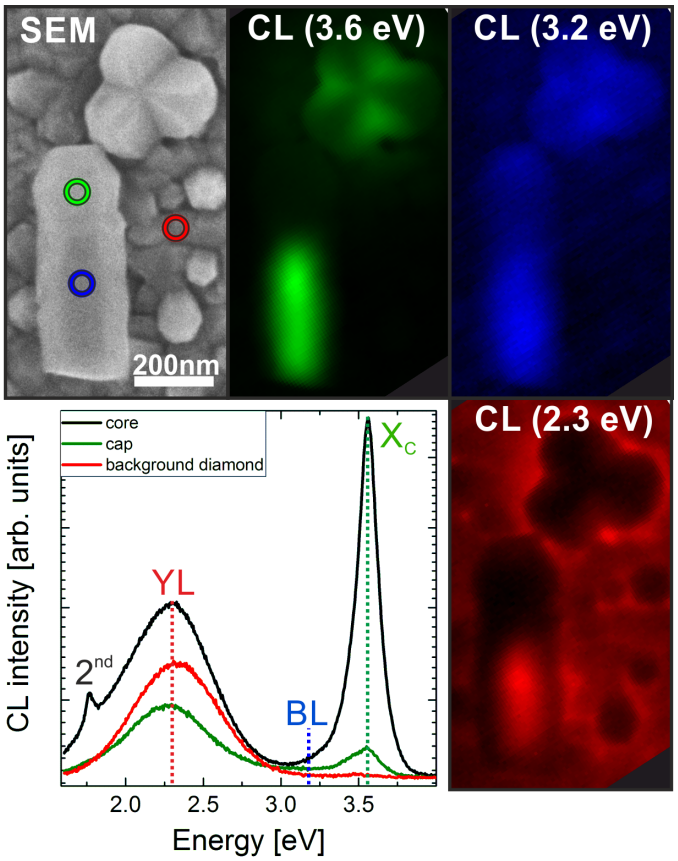

Fig. 4 SEM image, CL maps and CL spectra of distinct sites along a GaN-(Al,Ga)N core-shell NW grown on diamond substrate. The colored circles in the SEM image indicates the sites where the CL spectra have been recorded. The CL maps are at an equivalent sites and refer to different spectral emissions. 'Green' refers to 3.6 eV, 'Blue' and 'red' correspond to 3.2 eV and 2.3 eV, respectively.

particular mask hole.[2] The CL maps of the same region are colored according to different emission energies. In particular, 'green' corresponds to the X_C emission at 3.6 eV, whereas 'blue' and 'red' refer to the BL (3.2 eV) and YL emission (2.3 eV), respectively. The X_C luminescence is characterized by a homogeneous intensity along the NW core (Fig. 4 black curve). Similar to core-shell NWs on Si, the X_C emission is still visible when exciting the (Al,Ga)N cap (Fig. 4 green curve). This has been assigned to absorption of emitted light from the (Al,Ga)N band gap and re-emission at the GaN/(Al,Ga)N interface. However, in contrast to Si substrates, no characteristic peak at the BL emission line can be identified. Instead, a slightly increased signal compared to the zero line indicates a minor presence of BL-related defect centers within the (Al,Ga)N. Note that the seemingly higher intensity of BL in the CL map (3.2 eV) of the GaN core is due to the influence of the X_C emission line in this region. In the case of the YL emission (Fig. 4, 2.3 eV CL map), the signal is pronounced within the GaN core (Fig. 4 black curve), but also on the diamond substrate overgrown by (Al,Ga)N (Fig. 4 red curve). Noticeable is the reduced YL emission for thick (Al,Ga)N crystallites and also the (Al,Ga)N cap of the NW investigated (Fig. 4 green curve).

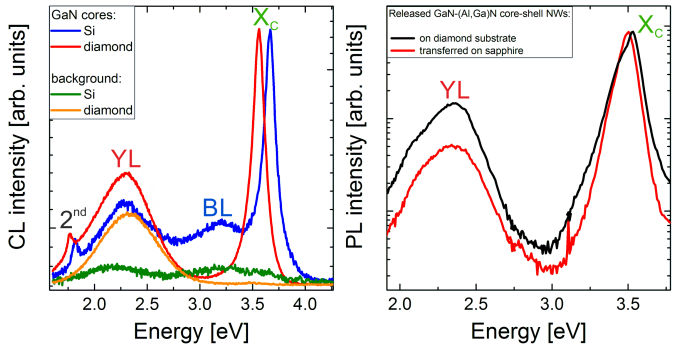

Fig. 5 (Left) CL spectra of the GaN cores and the background signal of the substrates for GaN-(Al,Ga)N core-shell NWs grown on Si and diamond. (Right) PL spectra of GaN-(Al,GaN) core-shell NWs lying on their original diamond substrate and of transferred NWs on sapphire.

For a direct comparison of the YL emission on both substrates, i.e. diamond and Si, the corresponding CL spectra of the GaN cores and the substrate background signals are plotted in Figure 5 (left). The YL intensity of the CL spectra obtained on the diamond substrate (Fig. 5 left, orange curve) is distinctively higher than on the Si substrate (Fig. 5 left, green curve). In particular, the emission measured on Si is slightly above the zero level and can, thus, be assigned to an interfering signal from core-shell NWs in the vicinity of the measurement spot. In contrast, a pronounced YL emission has been obtained from everywhere on the diamond substrate, whereas highest intensities have been measured directly around large nucleation spots, e.g. parasitic (Al,Ga)N crystallites, core-shell NWs or tripods (Fig. 4, 2.3 eV CL map). We attribute this discrepancy of the YL emission of the different substrates to an additional emitter in the diamond substrate. In particular, N-related point defects such as NV, H3 or N3 centers in the diamond crystal lattice show broad emission spectra between 1.9 and 2.5 eV.[3] Thanks to a similar refractive index of both diamond and (Al,Ga)N in this spectral regime and the waveguide geometry of as-grown core-shell NWs and (Al,Ga)N crystallites, an efficient outcoupling of light from the diamond can occur. As this diamond-related luminescence superimposes the YL emission from the GaN core, a convincing evaluation of the YL-related defects in core-shell NWs grown on diamond is not possible for this sample configuration.

In order to address this, GaN-(Al,Ga)N core-shell NWs grown on diamond substrate have been transferred on a sapphire substrate. In Figure 5 (right) exemplary PL spectra of an ensemble of NWs lying on their original diamond substrate and NWs transferred on a sapphire are plotted. Note that the intensities are normalized on the X_C emission for a better comparison. The YL intensity of the transferred NWs is distinctively lower compared to NWs lying on the diamond substrate. In particular, PL measurements of different NWs has revealed a reduction of YL by 50-65% for the transferred NWs. This proves a significant contribution of the diamond substrate on the YL emission. As a consequence, the YL emissions of core-shell NWs on both Si and diamond substrates show a similar YL emission, whereas the BL emission is strongly reduced on diamond.

5 Electron dispersive X-ray spectroscopy of a GaN-(Al,Ga)N core-shell NW

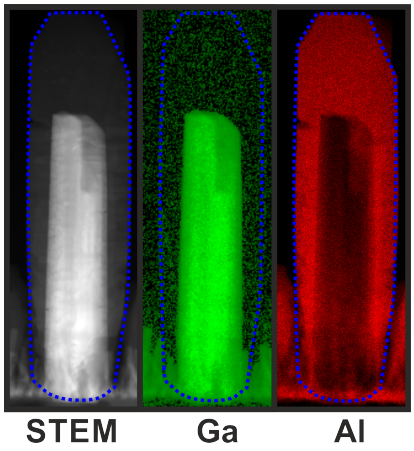

Fig. 6 Cross-sectional STEM image of a GaN-(Al,Ga)N core-shell NW grown on Si substrate with corresponding false-colored EDX maps of the atomic species Ga (green) and Al (red). As a guide to the eye, the core-shell NW is indicated by blue dashed lines.

In the CL measurements of GaN-(Al,Ga)N core-shell NWs on Si, the GaN-related YL defect emission has been identified when exciting the (Al,Ga)N cap. In order to identify possible GaN clusters as the origin for this emission, electron dispersive X-ray spectroscopy (EDX) has been performed in a scanning transmission electron microscope (STEM). In Figure 6, a cross-sectional STEM image of a thinned GaN-(Al,Ga)N core-shell NW together with EDX maps revealing the atomic species Ga and Al are shown. No Ga-rich inclusions within the shell could be observed. In contrast, almost no Ga has been detected within

the shell. As YL can only be emitted from extended GaN crystals, alloy fluctuations of the shell can be excluded to be the reason for the observed YL in CL during excitation of the (Al,Ga)N cap. In contrast, an absorption and re-emission of the (Al,Ga)N band gap luminescence of the GaN core seems to be the remaining plausible explanation.

6 TEM images of GaN-(Al,Ga)N core-shell NWs with thicker cores

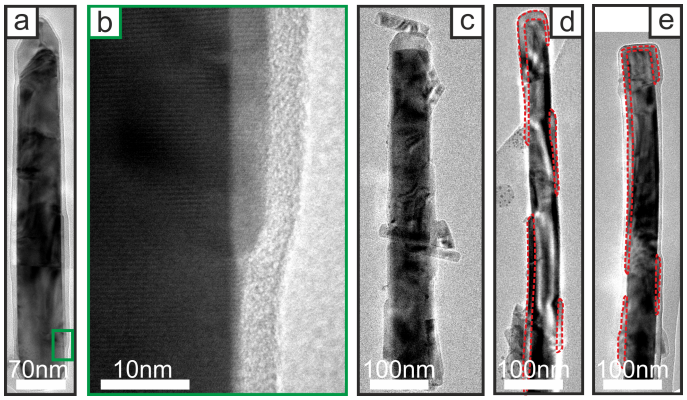

Fig. 7 (a) Cross-sectional TEM image of a GaN-(Al,Ga)N core-shell NW with a thicker core diameter of 64 nm after 3' shell growth. (b) High magnification image of a distinct location along the NW side facet of (a). The outer amorphous layer is assigned to contamination due to the NW dispersion. (c) Cross-sectional TEM image of a core-shell NW showing a cracking of shell nuclei. (d,e) Different core-shell NWs with a thinner core.

In Figure 7a a cross-sectional transmission electron microscopy (TEM) image of a GaN-(Al,Ga)N core-shell NW with a core diameter of 64 nm and a shell growth time of 3', i.e. during the shell nucleation stage, is shown. In contrast to the core-shell NW with smaller diameter of 40 nm (in the main article), a bowing of the NW along the growth axis has not been observed here. An investigation of numerous NWs indicates that the shell crystallites show a trend to be more extended along the side facets compared to smaller core diameters. Moreover, the average shell thickness observed after this growth time is distinctively smaller compared to thinner cores. For this particular NW, a maximum shell thickness of 4 nm has been measured (Fig.7b) whereas shells with thinner cores show thicknesses around 6.5 nm. These observations are in agreement with the proposed strain-mediated nucleation model: Due to the larger core diameter, less strain is occurring within the GaN core so that no significant bowing is present. As a consequence, the lattice parameters of the core are more uniform along the NW despite (Al,Ga)N nucleation which leads to an undisturbed growth of the separate shell crystallites along the side facets. However, due to the effectively higher lattice mismatch between the GaN core and the (Al,Ga)N shell the growth rate of the shell decreases which results in a decreased shell thickness for larger GaN cores.
During TEM measurements it has often been observed that shell nuclei (in their nucleation stage) lift off the core-shell structures

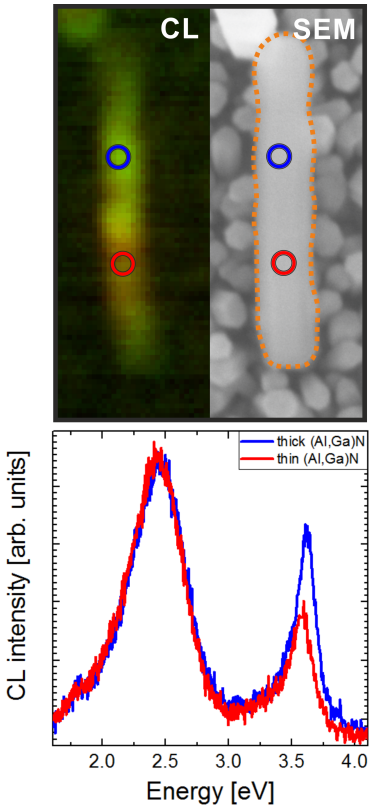

Fig. 8 Room temperature CL spectra of a GaN-(Al,Ga)N core-shell NW thin and thick (Al,Ga)N shell segments along the growth direction with corresponding false-colored CL map and SEM image of the NW.

in the case of thick cores (Fig.7c). The enhanced strain within the (Al,Ga)N shell in combination with the NW releasing process onto the TEM grid seems to destabilize the nuclei, leading to a cracking of the heterointerface.
In order to substantiate the proposed nucleation mechanism of the (Al,Ga)N shell in the main article, TEM images of two additional core-shell NWs with a thin core are displayed in Figures 7d and 7e. Similar to the core-shell NW with a thin shell in the main article, a bowing and an opposing assembly of the (Al,Ga)N crystallites on each side can be observed.

7 CL analysis of a GaN-(Al,Ga)N core-shell NW with a thin shell

In Figure 8 CL spectra of a GaN-(Al,Ga)N core-shell NW, released from a Si substrate, with a lower shell growth time of 9' is displayed. Due to the initially inhomogeneous nucleation of the (Al,Ga)N shell crystallites, a variation of the shell thickness and a slight bowing of the NW can be observed in the SEM image. According to the CL measurements the local degradation of strain at a thin shell site leads to both a redshift and a pronounced intensity quenching of the GaN X_C emission line. In contrast, the YL signal remains constant and is even higher in intensity compared to X_C. A BL emission can not be observed for these thin shells. Thus, a sufficiently thick shell seems to be required to effectively passivate the YL defect emission (Fig. 3a). The

reduction of X_C intensity at thinner shell parts is in agreement with the measurements on a cone-shaped NW in the main article.

References

1 S. Birner, T. Zibold, T. Andlauer, T. Kubis, M. Sabathil, A. Trellakis and P. Vogl, *IEEE T. Electron Dev.*, 2007, **54**, 2137–2142.

2 F. Schuster, M. Hetzl, S. Weiszer, J. A. Garrido, M. de la Mata, C. Magen, J. Arbiol and M. Stutzmann, *Nano Lett.*, 2015, **15**, 1773.

3 S. Pezzagna, D. Rogalla, D. Wildanger, J. Meijer and A. Zaitsev, *New J. Phys.*, 2011, **13**, 035024.